International Journal of Advanced Technology and Engineering Exploration, Vol 9(92)
ISSN (Print): 2394-5443 ISSN (Online): 2394-7454
http://dx.doi.org/10.19101/IJATEE.2021.875348

Research Article

Monitoring volcanic activity of Barren Island, India using multi-sensor and thermal remote sensing

A. Rajani[1*] and S. Varadarajan[2]
Research Scholar, Department of Electronics and Communication Engineering, Sri Venkateswara University College of Engineering, Sri Venkateswara University, Tirupati, Andhra Pradesh, India[1]
Professor, Department of Electronics and Communication Engineering, Sri Venkateswara University College of Engineering, Sri Venkateswara University, Tirupati, Andhra Pradesh, India[2]

Received: 20-December-2021; Revised: 10-July-2022; Accepted: 12-July-2022

Abstract
The usage of thermal remote sensing to perceive active volcanoes is relatively a new approach. Volcanic activity is always present when heat is transferred from the Earth's surface layer into the air. This thermal anomaly may be perceived using remote sensing and which is a quick approach to detect volcanic activity. Active volcanoes are detected using satellite thermal data, which is also used to anticipate eruptions and display drifts and forms at the time of eruption disasters. The goal of this study is to keep track on India's only stravo-volcano, Barren Island volcano (BIV), which has been active since 1991 with reference to thermal activity. The BIV's land surface temperature (LST) is monitored using Landsat 8 thermal infrared (TIR) data to detect eruptions and track thermal activity. When clear images of Landsat 8 are not possible during an eruption, Sentinel-2 data is used to identify volcanic eruption features like, lava flow, ash plume, and direction of lava flow from the cinder cone by visual interpretation. For the development of global volcanic monitoring, it is critical to combine different satellite data. Based on numerous satellite data and observations, BIV activity was studied throughout the active period from January, 2017 to March, 2021. Here, the two eruptive phases of January-March, 2017 and September, 2018 to January, 2019 were considered. Middle infrared observation of volcanic activity (MIROVA) system estimates volcanic radiative power (VRP) using moderate resolution imaging Spectroradiometer (MODIS) sensor data and radiant flues of the volcanoes have been presented in the web resource www.mirovaweb.it. This database was utilized by the current research work to validate LST estimated by using a mono-window algorithm based on Landsat 8 data. In addition to that, thermal anomaly in the form of fire pixel temperature values was estimated and made available to public in national aeronautics and space administration's (NASA) fire information for resource management system (FIRMS) database. The temperature data which is available in the NASA's FIRMS was used to compare estimated LST values at the study location BIV using high spatial resolution Landsat 8 data. FIRMS uses visible infrared imaging radiometer suite–band 14 (VIIRS-14) sensor data to estimate fire pixels temperature values. Suomi national polar-orbiting partnership (NPP) spacecraft of NASA and national oceanic and atmospheric administration-20 (NOAA-20) spacecraft carry VIIRS sensor. Finally, morphological changes and thermal deviations in topical eruptive episodes of the BIV were deliberated using multi-sensor, multi-temporal and multi-resolution data from various portions of the radio-frequency spectrum. From the results it was observed that, estimated LST values and Sentinel-2 based false colour composite (FCC) images can have the ability to predict the thermal changes occurring at active volcanoes.

Keywords
Barren Island volcano (BIV), Landsat 8, Sentinel-2, MODIS, LST, VRP, MIROVA, VIIRS.

1.Introduction
Volcanic eruptions are nature's most powerful force. Volcanic eruptions can be far more powerful than even the most powerful nuclear detonation. Volcanoes have killed thousands of people and triggered some of the world's most terrifying events [1].

On the internet, images of molten lava spewing from volcanoes are thrilling to behold.

The usage of thermal remote sensing to perceive active volcanoes is relatively a new approach. Volcanic activity is always present when heat is transferred from the Earth's surface layer into the air. This thermal anomaly may be perceived using remote sensing and which is a quick approach to detect

*Author for correspondence

volcanic activity. Active volcanoes are detected using satellite thermal data [2]. It is also used to anticipate eruptions and display drifts and forms at the time of eruption disasters. Volcanoes fortunately, exhibit precursory disturbance when that was identified and examined in time, allows for the early prediction of eruptions to pass the warning to communities at risk [3]. These precursors provide no information about the nature or scale of an upcoming eruption (that information is best obtained by mapping previous eruptions) [4, 5]. Precursors might last for weeks, months, or even years before erupting, or they can fade away at any time without being followed by an eruption. For more than 60 years, the Campi Flegrei volcano in Italy has been showing signals of disturbance. The lead-up time to volcanic eruptions usually gives affected communities enough time to prepare response plans and mitigating measures [6]. Remote sensing is being used to digitally monitor over 1400 potentially active volcanoes across the world. Volcanic activity is measured using active radar sensors, passive optical sensors, and thermal sensors [7]. In a broad sense, remote sensing of volcanoes entails monitoring volcanic activity without relying on in-situ observations, as well as taking into account data and observations from seismological [8] and global positioning system (GPS) networks. As a result, remote sensing is the key to understand how the Earth's volcanoes work, as well as why, when, and where they erupt.

Volcanoes can have an impact on the weather and climate of the Earth. Cooler than normal temperatures were recorded worldwide following the 1991 eruption of Mount Pinatubo in the Philippines, and brilliant sunsets and sunrises were attributed to this eruption, which ejected fine ash and gases into the stratosphere, resulting in a massive volcanic cloud that travelled around the globe. About 22 million tonnes of sulphur dioxide (SO_2) in this cloud interacted with water to form sulfuric acid droplets, blocking some sunlight from reaching the Earth and reducing temperatures in some areas by up to 0.5 degree Celsius [9]. Recently on 15 January 2022 Hunga Tonga-Hunga Ha'apai Volcano of Tonga Island erupted aggressively by releasing Sulphur Dioxide mass was ~ 0.4 Tgms (Terro grams) based on TROPOspheric monitoring instrument (TROPOMI) satellite based SO_2 measurements. Based on the simulation results it was estimated that the global mean surface temperature may decrease by 0.004 degree Celsius in the first year [10].

Monitoring active volcanoes entails real-time data collection via remote sensing and analysis of diverse data, such as earthquakes, ground movement, gas emissions, and atmospheric wave's data obtained using ground based and space-based instruments [11, 12]. Consider the September 2010 eruption of Indonesia's Mount Merapi volcano; it was an avalanche visible to the south of the peak a few days later, with white plumes rising over the crater. In March, a lava dome was discovered, and it quickly grew. The Indonesian center for Volcanology and geologic hazard mitigation (CVGHM) invited support from the volcano disaster assistance program (VDAP) to intensification of volcano watching. VDAP provided, satellite radar data and that was particularly useful in tracking Mount Merapi's 2010 eruption. As a result of the eruption's foresight, almost 70,000 individuals were successfully evacuated [13].

Volcanic monitoring is seen by scientists as a form of never-ending learning, in which the more the data collected, the better interpretation of volcanic progressions in evolution and the potential to predict forthcoming venting impacts [14]. One of the most reliable sources of information in this regard is remote sensing data from space, which is primarily used to monitor the huge number (50%) of vigilantly vigorous volcanoes (1400) that lack typical ground-launched equipment [15]. Even for volcanoes that were supervised by satellite data can provide a spatiotemporal observation of outbreaks, filling in the gaps left by ground-based monitoring [16].

Active volcanoes will be monitored by a number of organizations like, the world organization of volcano observatories (WOVO), global volcanism program (GVP) by the Smithsonian Institution National Museum of Natural History; middle infrared observation of volcanic activity (MIROVA) is a collaborative project between the Universities of Turin and Florence (Italy), Alaska Volcano observatory etc. Volcano observatories organise the scientific information needed to respond to volcanism in order to effectively communicate with the authorities responsible for civil protection. Planning in advance is essential to ensure that the observatory has the data, tools, and computer systems necessary to support decision-making. Construction of monitoring networks is heavily influenced by the hazard posed by a region or country's concentration of volcanoes [17]. To examine the relationship between regional seismicity and volcanoes, earthquake data and Volcanic radiative power (VRP)

data were used. It has been observed that the frequency of earthquakes has increased following / before the volcanic eruption. The frequent earthquakes are thought to indicate a release of pressure, which leads to looseness in the area, resulting in volcanic outbursts or at least variation of the outbreak [18].

The motivation for choosing Barren Island volcano (BIV) is that, India's live volcano in the Andaman and Nicobar Islands erupts now and then after 2005. According to an Indian space research organisation (ISRO) scientists study it was observed BIV eruption after 26 December 2004 Indian Ocean earthquake and tsunami near Sumatra, Indonesia. Volcanic eruptions in Sulawesi, Indonesia, were observed and linked to earthquakes on September 28, 2018[12, 16]. With the above all observations, it is required to ensure continuous monitoring of this BIV eruption. So this research work considered one of the ways to monitor volcanic eruption by means thermal remote sensing. It has been recently erupting with such ferocity. According to authorities at the National Institute of Oceanography (NIO) in Goa, the BIV resurfaced in 1991 after being dormant for almost 150 years. Now it has begun spewing ash once more.

Several historical eruptions were detected between 1787 and 1832 on Barren Island, an unpopulated island found North-East of Port Blair, the capital of Andaman and Nicobar islands. There was no more sign of activity up to 1991, when Strombolian explosions, dust clouds and lava tides were discovered when they reached the sea. Similar eruptions have happened on a regular basis since 2005, lasting months to years [19]. Ground based observations are rare due to the volcano's remoteness. According to satellite data and reports from the Darwin volcanic ash advisory centre (VAAC), an eruption began in September, 2018 and lasted till early 2019, with occasional thermal anomalies. This information from the Source: www.volcano.si.edu and specifically: https://volcano.si.edu/volcano.cfm?vn=260010.

Global multispectral and thermal band datasets will be provided by satellite-based sensors such as the advanced land imager (ALI) on earth observing one (EO-1), the moderate resolution imaging spectroradiometer (MODIS) on the TERRA/AQUA satellites. And these datasets are used by the most volcano observatory organizations [20, 21] to monitor unrest volcanoes. The advanced spaceborne thermal emission and reflection radiometer (ASTER) and thematic mapper (TM), enhanced thematic mapper plus (ETM+), thermal infrared sensor (TIRS) are the well-known Landsat series sensors used to determine the thermal character of lava drifts throughout outbreak episodes [22, 23]. Volcanic eruptions linked to deformation or settling has been successfully monitored using other remote sensing methods, such as Interferometric synthetic aperture radar (InSAR) [24].

Landsat-8 data will be the greatest option for determining land surface temperature (LST) and spotting thermal anomalies, but due to its lower temporal resolution than MODIS sensors, it has some drawbacks. Finer spatial resolution, on the other hand, is a huge benefit, as it aids in the compilation of high-quality data, which is especially useful for monitoring volcanic eruptions based on previous eruption data analysis. For the volcano monitoring team, thermal infrared (TIR) remote sensing techniques are unquestionably a feasible option for monitoring and analysing geothermal systems as well as extraordinary occurrences such as volcanic eruptions. While cloud cover and revisit cycles can be an impediment, simple methods for processing high-quality data can be a tremendous help [25].

The system MIROVA uses MODIS sensor data to automatically detect volcanic radiations. The system can detect, confine and measure thermal abnormalities in near real-time by giving infrared pictures and thermal fluidity time-series data on over 200 volcanoes around the world on a committed website (www.mirovaweb.it) [26]. Because of the increasing accessibility of open source records by space organisations, the publication and involvement of satellite data/products has become a support of open research in volcanology with the beginning of the new millennium and the expansion of the internet [27−29].

LST is one of the key parameter to study about the characteristics of land processes that are related with interactions between the earth surfaces, the atmosphere and the energy balance [30]. LST values change continuously over time and space, assessing its variation can reveal unknown processes and is of great importance to numerous applications [31]. The LST is usually used in multiple fields, including climate change, evapotranspiration, hydrological cycle, vegetation monitoring, drought, forest fires, urban climatology, environmental studies, volcanic monitoring and so on [32, 33]. LST retrieval using TIR sensor remote sensing has increased over the

years and a number of algorithms developed. To estimate LST using TIR sensor data from satellite needs to consider many parameters like radiometric and atmospheric calibrations. It can be assumed, under this land surface classification framework, that the LST difference is mainly caused by various landscape compositions, shapes, and spatial arrangements [34].

However, there is evidence that MODIS data can be used to monitor active volcanoes. The main applications of Landsat 8 datasets include crop-based applications, soil moisture analysis, vegetation monitoring, and climate change monitoring [35]. The Landsat series satellite temperature data are given less weight for monitoring volcanic activity. It could be because its high temporal resolution (less frequently) the data is available. According to scientific standards, monitoring and forecasting volcanic eruptions must take into account historical data in addition to the data currently available. As a result, this research examined extracting thermal data from Landsat 8 datasets and comparing it with the database from the resource MIROVA system and national aeronautics and space administration (NASA) based fire information for resource management system (FIRMS) system. The best resolution of Landsat datasets is the primary justification for consideration.

The current study's objective is to evaluate the currently active volcano BIV by finding thermal anomalies using Landsat 8 datasets. Also, by visually inspecting morphological changes during a volcano eruption using Sentinel-2 satellite datasets. The mono window algorithm is used to calculate LST at the study area using Landsat 8 datasets [36]. The obtained results were validated using data from the MODIS satellites, which may be obtained from the MIROVA system database available at web resource www.mirovaweb.it. VRP was used to illustrate thermal anomalies [37]. The "fire" pixel data from NASA's FIRMS database can be utilized to compensate for the lack of in-suite observations to compare with obtained results.

The remainder of the paper is structured as follows: The literature review for the on-going research is presented in Section 2. The BIV, which was selected as the study region for observing volcanic activity, is the subject of Section 3. Additionally, a block diagram was used to demonstrate the suggested research work methodology to track volcanic activity in this area. Furthermore, LST estimation using a mono - window algorithm is described here with a flow chart and algorithmic steps. The output results attained by using image processing methods through aeronautical reconnaissance coverage geographic information system (ArcGIS) 10.3 software were displayed in Section 4. Discussions were given here based on the results of the analysis. Finally, in Section 5, conclusions and future scope were offered based on the outcomes, observations and discussions.

2.Literature review

Gunda et al. [38] presented the detailed report on the need to monitor and know the volcano dynamics with respect to seismicity at BIV using multispectral datasets, volcanic radiative power (VRP) data about 20 years and earthquake historical data (1950–2020 July) ~70 years. From this study it was observed that, in comparison to 1950–1989, the rate of earthquake frequency increased to 3.54 times between 1990 and 2020, indicating seismicity-induced pressure release that may have produced decompression in the region, resulting to eruptions or at least modulation of the eruption. They concluded that, volcanic activity related to earthquake seismicity.

Coppola et al. [39] provided a detailed study report on www.mirovaweb.it a dedicated web facility for monitoring active volcanoes. The main aim of the MIROVA system is to continuously monitor and update data on over 200 active volcanoes across the world. It will carry out the task using data from MODIS sensor and Sentinel satellite. Currently, four basic types of remote sensing observations (RSO) are used to gain a better knowledge of the main processes that occur inside a volcanic system. These are i) from microwave band; ground distortions (ii) from the ultraviolet and infrared band; SO2 degassing (iii) from infrared band ash release and finally (iv)heat flux from infrared band. This MIROVA data is now being used for research work to monitor active volcanoes. The researchers who were working on active volcanoes will refer this web resource. The MIROVA data was also used in this study to analyse the results obtained.

Blackett [40] had done first observation of volcanic activity using Landsat8 on 29 April 2013 (just two weeks after its launch). It has been shown to provide useful quantitative data relating to the activity of the volcano at the time. Once the TIRS band 11 calibration issues are resolved, the satellite's two thermal bands can be used to apply split-window algorithms, something that has never been possible with only one TIR band on previous Landsat

satellites, and to generate a time-series of observations from which varying lava effusion rates can be calculated more accurately than with just one image.

Flynn et al. [41] presented how effectively active volcanoes can be monitored using Landsat7 ETM+ sensor data of Panchromatic and thermal images having 15m and 60m resolution respectively. Here comparison did with the 4km resolution satellite datasets. Landsat 7 offers value-added enhancements over its Landsat 4 & 5 series satellites. It was possible to map lava flow fields, follow very high temperature lava channels, and locate an arcuate feature linked with a collapsed crater floor at Lascar volcano, a behaviour that may presage explosive activity, using panchromatic data. They can trace the branching and braiding of subsurface lava tunnels at Kilauea volcano.

Ramsey and Harris [42] Presented detailed review report on volcanology 2020. They considered only on thermal infrared remote sensing of surface activity using ground-based and space-based technology and the subsequent research results. This review addressed remote sensing usage in future for thermal anomalies of volcanoes. They did not address the application of remote sensing to the entire field of Volcanology.

Ramsey and Flynn [43] considered the study area tatun volcanic group (TVG), Taiwan. The LST and radiative heat flux (RHF) were retrieved using the Landsat 7 ETM+ imagery, while MODIS 8-day average LST products were utilised to monitor the TVG's Jinshan fault zone. The occurrences of hot springs and fumaroles follow the LST anomaly distribution, and the total temperature in the E-W ridge is greater than the SW-NE ridge in TVG, according to validated results. They also concluded that, the volcanic activities (i.e., movement of magma) underneath Tatun Volcanic Group can be the major cause of earthquakes.

Silvestri et al. [44] considered ASTER and Landsat8 datasets for the study of thermal anomalies at Volcano Island, Italy. Landsat8 band10 data was used to retrieve the LST. Here the correlation between the in-suite surface temperatures obtained from pyrometer and thermocouple and LST from Landsat 8 done. It was observed by them that, values with those acquired by field and airborne measurements close-fitting differences of about 5% with the night-time acquisition and up to 50% with daytime acquisition.

Marchese et al. [45] developed multi-channel algorithm for monitoring thermal anomalies using Landsat 8 OLI data and Sentinel-2 MSI datasets. Normalized hotspot index (NHI) computed using both the short wave infrared (SWIR) and near infrared (NIR) band data obtained from MSI and OLI sensors. From the results it can be concluded that, NHI has the potential to map both weak and intense volcanic thermal anomalies. This algorithm was suitable for daylight images. The performance of algorithm improved by using certain tests for cloud covered images. This algorithm was sensitive to fire pixels, so spatial distance filters were used to avoid misinterpretation.

Layana et al. [46] developed a new, low-cost and semi-automatic online system based on Landsat 8 images. This system was named as volcanic anomalies monitoring system (VOLCANOMS) and its web resource: https://volcanoms.ckelar.org. It uses various bands like NIR, SWIR and TIR for thermal anomalies detection. Here authors presented the study report on following 5 active volcanoes Krakatau, Stromboli, Fuego, Villarrica and Lascar volcanoes. This VOLCANOMS tool developed using open source software Python. Volcanic image processing software (VIPS) is used for online processing of Landsat images. The files can be accessed from United States Geological Survey (USGS) earth explorer website https://earthexplorer.usgs.gov/. The region of interest (ROI) can be selected manually. https://search.earthdata.nasa.gov/search?fi=ASTER used for surface emissivity of a specific volcano. https://atmcorr.gsfc.nasa.gov/ used for obtaining transmissivity for a specific day and time of single volcano.

Xiang et al. [47] proposed morphological changes identification using Sentinel-1 images and advanced land observation satellite-2 (ALOS-2) satellite images using optical images. The area to change detection and progress were tested and evaluated by combing the results from synthetic aperture radar (SAR) and optical data. Study area chosen for morphological changes at Anak Krakatau, Indonesia. Based on 22 December 2018 volcanic eruption pre and post eruption images were considered for the interpretation of morphological changes. As optical images are affected by clouds and fog, here synthetic aperture radar (SAR) images were considered. Sentinel-1 dual-polarized water index (SDWI) and

the Nobuyuki Otsu (OTSU) polarization method used for extraction of volcanic morphology at Anak Krakatau, Indonesia.

Cho et al. [48] proposed a machine learning algorithm to reconstruct LST using MODIS data with all-sky cases having 1 km resolution. Area considered for study was South Korea. The algorithm was light gradient boosting machine (LightGBM) approach which considers the cloud effects on LST. LST reconstruction was executed using MODIS data, output of local data assimilation and prediction system (LDAPS), in-situ data. This method considered two cases of cloud conditions one clear sky and another cloudy sky. The proposed method achieved more coefficient of determination in the daytime than nighttime for both the cases of clear sky and cloudy sky. The overall results show that, proposed light gradient boosting machine algorithm has obtained higher accuracy compared to LDAPS model.

Biggs et al. [49] suggested the need to monitor inactive volcanoes over decades to centuries with no historical records of eruptions. This baseline monitoring used to detect the early stages of reawakening of volcanic activity. Here Sentinel-1 five years data having ~ 5000 images of Turkey's volcanoes have been analysed using deep learning techniques. From results it was identified that, no cm-scale volcano deformation in Turkey since 2015 to 2020. So it was suggested to monitor volcanoes using InSAR technique.

3.Materials and methodology

3.1Study Area

Barren Island is a remote island east of India in the Andaman Islands. BIV is located on Barren Island. It is the only volcano that has been proved to be active in the Indian subcontinent. BIV is the only one in the chain of volcanoes that stretches from Sumatra to Myanmar. The research area can be located between the latitudes of 12° 17' 23" North and longitude 93° 52' 47" East. According to survey of India BIV can locate in the topographic sheet no. 86H/15 which covers the Barren Island. The island is located around 138 kilometers (86 miles) east-northeast of Port Blair town and has an area of roughly 8.3 square kilometers. It is part of the Andaman and Nicobar Islands which is part of Indian Union Territory. Within the Andaman Sea, it is 350 meters above mean sea level (MSL) and is made up of sporadic lava streams and pyroclastic deposits. Since prehistoric (unknown years) times, the volcano has shown "strombolian" style eruptions with ash emission and lava flow [50]. According to historic eruptive phases, the volcano was active between 1787 and 1832. In 1991, 1995, 2005-2007, 2008-2010, 2013-2016, and 2017 to present, there were sporadic eruptions with reference to data from the source:https://volcano.si.edu/volcano.Cfm?vn=260010. The location map of the study region is shown in *Figure 1*.

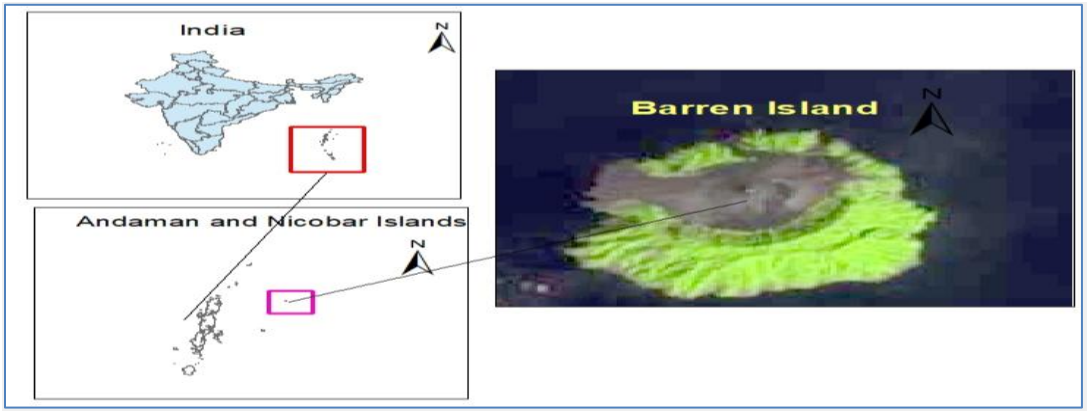

Figure 1 Study area map of barren island volcano

3.2Datasets

3.2.1Landsat 8

Landsat 8 was launched on 11-02-2013 by NASA in collaboration with United States geological survey (USGS) for earth observation facility. It consists of the two sensors onboard the operational land imager (OLI) camera and the TIRS. A global system i.e the worldwide reference system-2 (WRS-2) has been followed by Landsat 8 to catalogue scenes using path and row numbers. The size of each Landsat 8 scene will be 185 km x 180 km (114 mi x 112 mi). Seasonal coverage of the global continent is provided

by these two sensors at 30 metre spatial resolution (visible, NIR, SWIR bands), 100 metre spatial resolution (thermal band), and 15 metre spatial resolution (thermal) (panchromatic). The TIRS sensor of the Landsat 8 satellite senses surface temperature in two spectral bands at 10.6µm – 11.19 µm and 11.5µm – 12.51µm. When compared to TM and ETM+ sensor datasets of Landsat 5 and Landsat 7 respectively, which have only one thermal infrared band data. The thermal infrared band data is essential for tracking volcanic eruptions to lower risks and prevent calamities. Monitoring volcanoes with a satellite sensor can be classified into two categories: atmospheric and ground observation [51]. Monitoring eruptions, thermal anomalies, plumes, and ash clouds are examples of atmospheric observations that can be used to determine flight safety and the impact of volcanic eruption coverage. Ground monitoring on the other hand has a tremendous identification for mitigation, such as lava flow orientation and destruction [52]. The proposed research work exclusively uses LST estimates to monitor thermal anomalies and detect changes in temperature readings.

3.2.2 Sentinel-2

Sentinel-2 is the mission of the European space agency (ESA). It consists of two platforms: 2A and 2B, which were launched in June 2015 and March 2017 respectively. On-board technology gathers multispectral images with spatial resolutions extending from 10 to 60 metres, and 13 spectral bands ranging from visible to SWIR. Because of its revisit time of once every 5 days, it aims to track changes on the earth's surface. The Sentinel-2 satellite's datasets are widely used for continuous observation of vigorous volcanoes all over the world. The present study considered the SWIR1 & SWIR2 band with 20 m spatial resolution, as well as the blue, green, red, and near-infrared bands with 10 m spatial resolution with less than 10% cloud-cover images during the eruptive phase. Sentinel-2 Band 11 (SWIR-1), Band 12 (SWIR-2), and Band 2 (blue) band datasets were integrated to analyse geological changes at the volcano. *Table 1* displays the spatial data taken into account for the present investigation. Sentinel-2 A and B images were used in this research activity to visually evaluate thermal anomalies and identify morphological changes in the study area BIV.

Table 1 Spatial information about the study area

Data source	Sensor	Data	Spatial resolution	Bands considered	Path/ row
Landsat 8	OLI/TIRS	06-02-2017,	30 meters	B4 &B 5	133/52
		22-02-2017,	100 meters	B10	
		23-10-2018&			
		24-11-18			
Sentinel-2	Multi-Spectral Imager (MSI)	28/09/2018,	20 meters	B11, B12 & B2	N/A
		03/10/2018,			
		18/10/2018,			
		11/11/2020,			
		30/01/2021,			
		04/02/2021,			
		09/02/2021,			
		24/02/2021 & 01/03/2021			

3.2.3Terra and Aqua

Terra and Aqua are NASA's Earth observation satellites in a sun-synchronous orbit. While Aqua crosses the equator from south to north in the afternoon, Terra orbits the Earth from north to south in the morning. Both are equipped with a MODIS sensor, which will view the whole Earth's surface every one to two days. In 36 spectral bands with 250-1000 meter spatial resolution, MODIS collects data. Our knowledge of the dynamics and processes taking place on land, in the oceans, and the lower atmosphere will be enhanced by these data. To help policymakers make informed decisions about the conservation of our environment, MODIS is playing a crucial role in the creation of validated, global, interactive Earth system models. This research work considered the thermal band data of MODIS with a spatial resolution of 1000 meters. MIROVA system is an automatic "hot spot" detection system. It was created to identify, track down, and measure the source of heat radiation from volcanic activity [53]. VRP is the primary parameter calculated by the MIROVA system that represents the combined effect

of the “hot spot” area and its integrated temperature according to Stephan Boltzmann’s equation.

3.2.3.1MIROVA system

MIROVA is an automated system based on MODIS sensor data finds the unrest areas (hot spots) of active volcanoes and monitors its thermal anomalies. This sensor has a spatial resolution of 1km and a temporal resolution of 4 pictures per day. Despite its low spatial resolution, this sensor data has an excellent temporal resolution makes it ideal for catastrophe monitoring and hazard mitigation applications. This system uses "flag" to act on a limited number of target volcanoes (216) in response to requests from monitoring organisations. Each volcano on the planet is assigned a unique number by the global volcanism programme (GVP), making it easy to identify them. This technology can identify, localise, and measure thermal irregularities in near real-time by giving infrared image and continuous thermal irregularities data on over 216 volcanoes across the world into the web resource: www.mirovaweb.it . Several volcanic observatories are currently using the MIROVA system for daily monitoring, reporting, and also for research purpose [26]. In this work, the estimated LST values over the unrest period were compared with VRP log plots on specified dates and analysed using the database available on the MIROVA system (Resource: www.mirovaweb.it).

3.2.3.2Volcanic radiative power (VRP)

The VRP was calculated using middle infrared volcanic activity measurements to detect BIV thermal anomalies at high temperature more than 500K. VRP has been used to quantify the heat emitted by volcanic activity when satellite data was collected. The MIROVA method will be used to process these datasets, which are based on MODIS (level 1b radiances) data. The MIROVA system estimates the VRP parameter to detect thermal abnormalities at volcanoes [26]. It is calculated by taking into account the effect at the hotspot area (A_{hot}) as well as the temperature at the hotspot (T_{hot}). The law of Stephan Boltzmann’s, VRP = $\varepsilon*\sigma*$ A_{hot} * T_{hot} was used to calculate VRP. Where σ-Boltzmann’s constant and ε-emissivity.

3.2.4 Suomi NPP and NOAA-20

Suomi National Polar-Orbiting Partnership (Suomi NPP) and National Oceanic and Atmospheric Administration -20 (NOAA-20) satellites carry the Visible Infrared Imaging Radiometer Suite (VIIRS) sensor. It allows for daytime and night time the earth observation. The VIIRS sensor collects data in visible and infrared spectral bands around 22 channels. In that, 5 channels with 375 meters high resolution and 16 channels at 750 meters moderate resolution and it has a unique panchromatic Day/Night Band (DNB). NASA’s FIRMS distributes near-real-time (NRT) active fire data within three hours of satellite observation from NASA’s MODIS and VIIRS sensors. FIRMS system is part of the NASA’s Land Atmosphere Near real-time capability for earth observing system (EOS) land atmosphere near real-time capability for EOS (LANCE) (Source: https://www.earthdata.nasa.gov/ learn/find-data/near-real-time/firms). This FIRMS temperature values were compared with estimated LST values of the study area BIV for validating volcanic activity at the time of eruption phase.

3.3Methodology

The proposed research methodology takes into account data from several sensors to track the BIV for volcanic activity. *Figure 2* shows a block diagram of the proposed method used for monitoring volcanic activity at BIV based on various sensor data. Based on a survey of the literature, the current research project took into account different sensor data to monitor the BIV volcano based on thermal infrared data for temperature changes and optical data for morphological changes identification. Thermal remote sensing is essential for locating the "hot spots" during a volcanic eruption. First step is to estimate the LST using both OLI and TIR sensor datasets of Landsat 8. The reason to choose Landsat 8 data for the estimation of LST is due to its high spatial resolution. Due to its low temporal resolution (for every 16 days once revisit period) it’s not suggested to use Landsat 8 data for continuous monitoring mainly for the eruption period. Because of MODIS's great temporal resolution (1to 4 images per day), almost all volcanic monitoring systems rely on its datasets. The global volcanic program (GVP), MODVOLC algorithm, and MIROVA system automatically detects "hot spots" at volcanoes using MODIS sensor data [26]. This study used the VRP data from the MIROVA system as a reference to verify the LST calculated from the Landsat 8 data. Sentinel-2 images were originally taken into consideration for monitoring volcanic activity for visual inspection because they are available every five days. The morphological changes at the volcano BIV were also detected using Sentinel-2 A & B MSI sensor datasets by generating false colour composite (FCC) images. NASA's FIRMS temperature observations can be used to compare and validate estimated LST values.

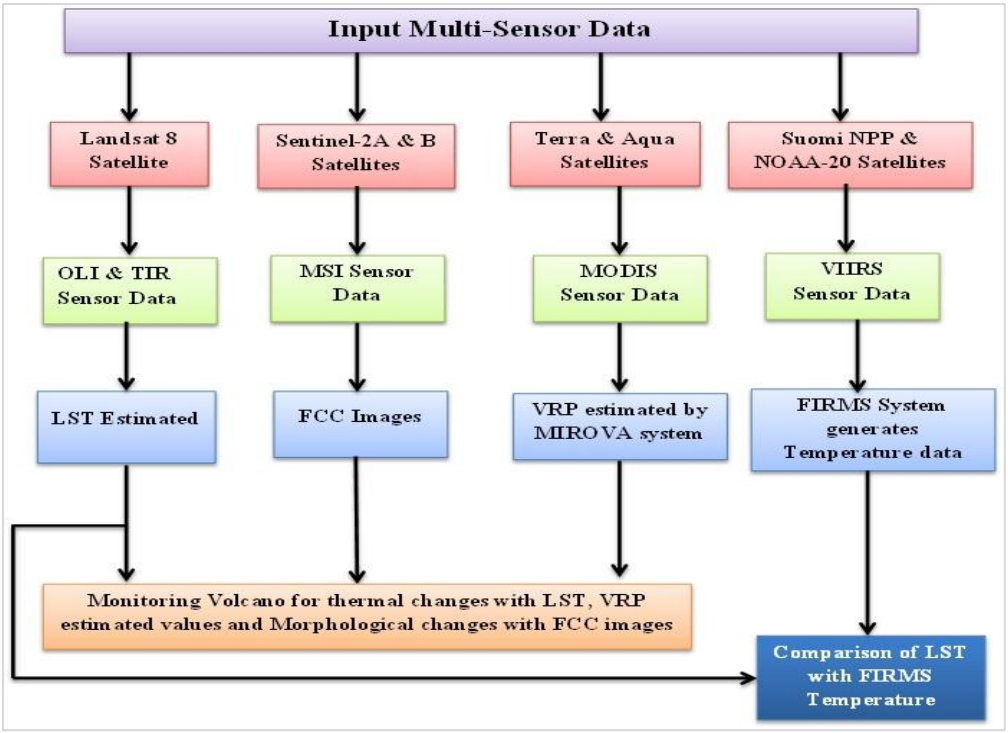

Figure 2 Block Diagram of the proposed method for monitoring volcanic activity at BIV

3.3.1LST estimation

This research work considered two active periods of BIV, which were January-March, 2017 and September, 2018 to January, 2019. Landsat 8 images with less than 10% cloud cover were examined from January 2017 to January 2019. One of the most significant parameters for monitoring and detecting volcanic activity is the LST. Land surface emissivity (LSE) has a big influence on LST measurements taken with remote sensing instruments, and atmospheric factors can skew the results. It is more accurate to estimate LST using the emissivity parameter, which will be determined using Normalized Difference Vegetation Index (NDVI) values (estimated using band 4 (red) and band 5 (near infrared) data). This study employs ArcGIS 10.3 software to analyse Landsat 8 spectral band datasets and to estimate LST. The LST of the research area was estimated using a mono-window algorithm [54]. For all band datasets, image pre-processing was done using the nearest neighbour technique with a pixel size of 30 X 30 m before applying the algorithm. The estimation process for LST is shown as a flowchart in *Figure 3*.

The processing steps for LST estimation using the Mono-Window Algorithm are as follows:

Step1: The transformation of image pixel values (i.e. digital number (DN)) into spectral radiance (L_λ) using Equation 1 gives top of atmosphere (TOA) (Top of Atmosphere).

$$L_\lambda = M_L * Q_{cal} + A_L - O_i \quad (1)$$

Where, L_λ denotes TOA's spectral radiance (mW /sr*m*m2); M_L - The value of multiplication rescaling can be found in the metadata file of the corresponding image; A_L - Additive rescaling element for every band from metadata file; Q_{cal} – Pixel digital number that have been quantized and calibrated; O_i - Adjustment factor

Step2: Using L_λ, K_1 and K_2, i.e. thermal constants provided in metadata, convert spectral radiance L_λ to Brightness Temperature (B_T). Equation 2 is used to calculate the brightness temperature in Celsius.

$$B_T = \frac{K_2}{ln\left[\left(K_1/L_\lambda\right)+1\right]} - 273.15 \quad (2)$$

Where B_T is the Brightness Temperature in degrees Celsius, L_λ is the TOA spectral radiance, and K_1 and K_2 are the Thermal Sensor constants from metadata.

If LSE was taken into account when utilising the mono-window algorithm approach for LST estimate, the average error might be reduced.

Step3: LSE (ε) parameter is dependent on vegetation proportion (P_v), which is based on normalized difference vegetation index (NDVI), and is measured by utilising band 4, and band 5 (Equation 3).

$$NDVI = \frac{(\text{Band5}) - (\text{Band4})}{(\text{Band5}) + (\text{Band4})} \quad (3)$$

Step4: The proportion of vegetation (Pv) is computed using Equation 4

$$P_V = \left(\frac{NDVI - NDVI_{min}}{NDVI_{max} - NDVI_{min}}\right)^2 \quad (4)$$

Step5: LSE (ε), which is predicted using the NDVI threshold approach. Because it is a proportionality thing, the LSE is required for computing the LST. It is used to scale blackbody radiance (Planck's law) in order to anticipate emitted radiance. It also has the capability of transferring heat energy from the surface to the atmosphere [36]. As a result, the emissivity of the land surface (ε) is calculated using Equation 5,

$$\varepsilon = \varepsilon_s (1 - P_v) + \varepsilon_v P_v + d\varepsilon \quad (5)$$

where, ε_v denotes Vegetation Emissivity Parameter, ε_s means Soil Emissivity Parameter, and P_v– Vegetation Proportion.

Equation 6 is used to compute emissivity (ε).

$$\varepsilon = 0.986 + 0.004 * P_v \quad (6)$$

where, the standard deviation (SD) of soil is 0.004, and the average emissivity is 0.989. (i.e vegetation & soil average emissivity).

Step6: Equation 7 is used to calculate LST in the last stage

$$T_s = \frac{T}{\left\{1 + \left[\left(\lambda T/\rho\right)\ln(\varepsilon_\lambda)\right]\right\}} \text{ °C} \quad (7)$$

Where,

λ - Wavelength of radiated light (10.8 μm); ε_λ - LSE and

$$\rho = h\frac{c}{\sigma} = 14388\ \mu m\ K \quad (8)$$

Where,

h=662.6 $\times 10^{-36}$ Js (Planck's Constant); c = 3×10^8 m/sec (Light Velocity); σ = 138 $\times 10^{-25}$ J/K (Boltzmann's Constant).

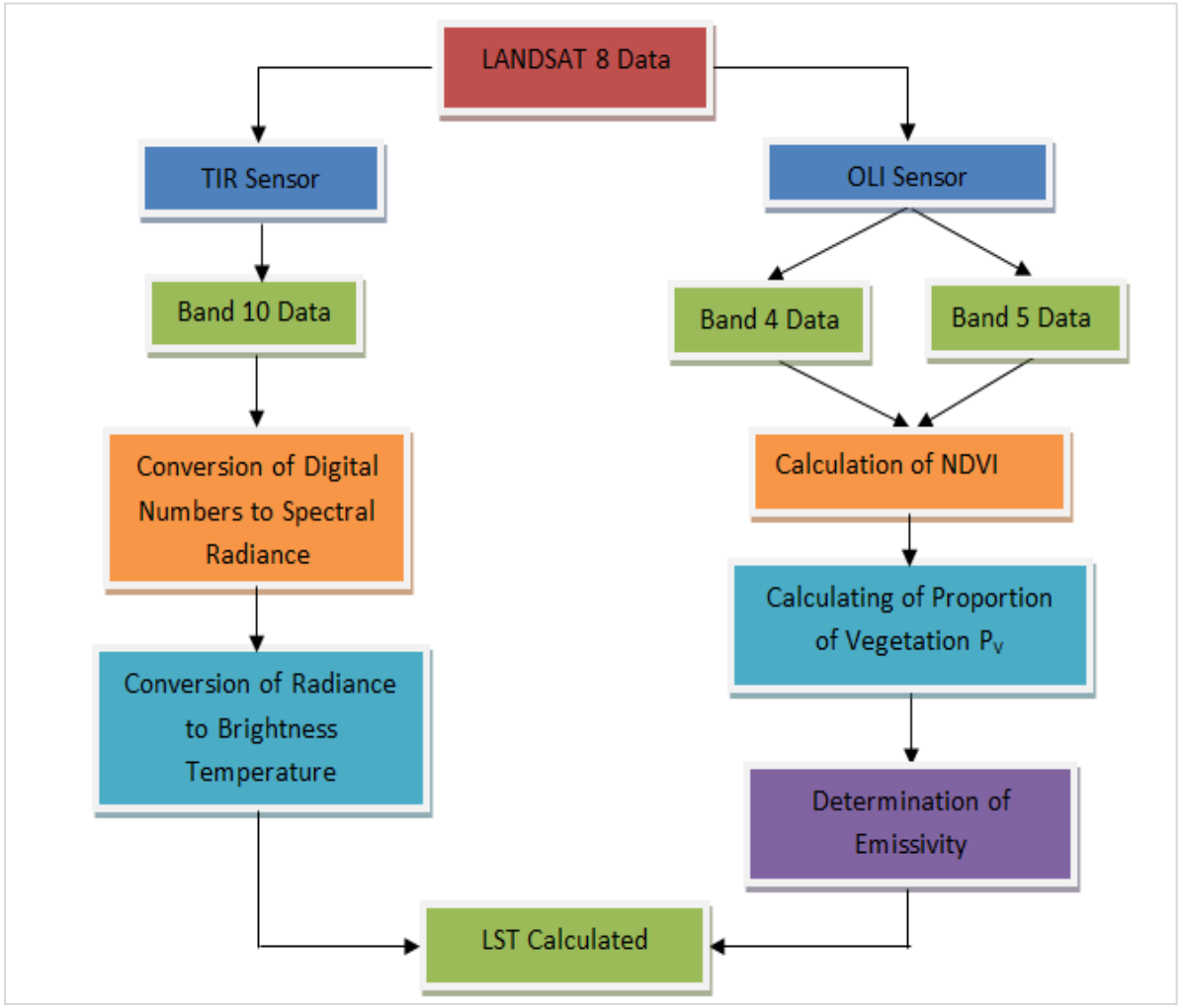

Figure 3 A flowchart for estimating LST

4.Results and discussions

4.1Landsat 8 datasets-estimated LST

According to the methodology section, the mono-window algorithm procedure, which entails six steps, was used to estimate the LST. Band 10 data was taken into consideration for LST estimates, although any of Landsat 8's thermal bands, such as band 10 or band 11, can be utilized to estimate brightness temperature. The two active phases of the BIV volcano are the focus of the ongoing research. Here, determining the LST values in the research area using Landsat 8 datasets and comparing such values to MIROVA system-based VRP products and VIIRS sensor based temperature values are the goals. Thermal band data or middle infrared band data from Landsat 8 datasets can be used to detect volcanic eruptions.

The eruptive stages taken into account here to track volcanic activity are January to March 2017 and September 2018 to January 2019. The LST maps created for the study area during the volcanic disturbance of January to March 2017 of BIV are shown in *Figures 4(a)* and *(b)*. LST is expressed here in degrees Celsius. *Figure 5* (a) depicts the log plot of the VRP obtained by the MIROVA system for the volcano BIV between November 2016 and November 2017 (Courtesy of MIROVA), and *Figure 5 (b)* displays the color coding applied to the VRP ranges. Yellow indicates low VRP, orange indicates moderate VRP, red indicates high VRP, and pink indicates extremely high VRP. *Figures 4(a)* and *(b)* show that the highest temperature recorded in 2017 was 65.47°C on February 6 and 47.86°C on February 22. It can be observed from *Figure 5(a)* that, the VRP value was high on February 6, 2017 and moderate on February 22, 2017. It can be inferred from the results that, Landsat 8 LST data are acceptable for identifying thermal anomalies by comparing the LST values calculated using Landsat 8 with the VRP values of the MIROVA system.

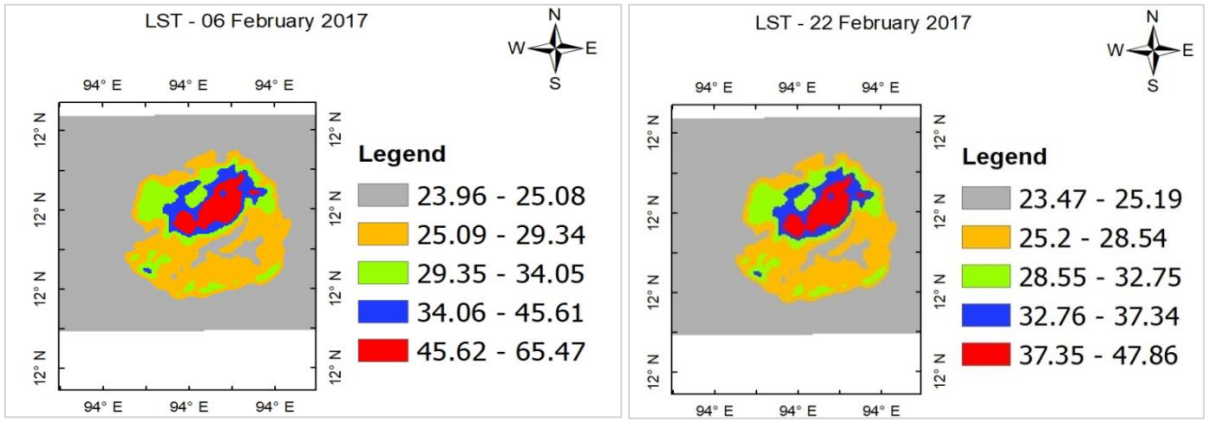

(a) (b)

Figure 4 (a) and (b) LST maps generated for the study area BIV for the volcanic unrest period January-March, 2017 by taking satellite images of Landsat 8 datasets from USGS earth explorer

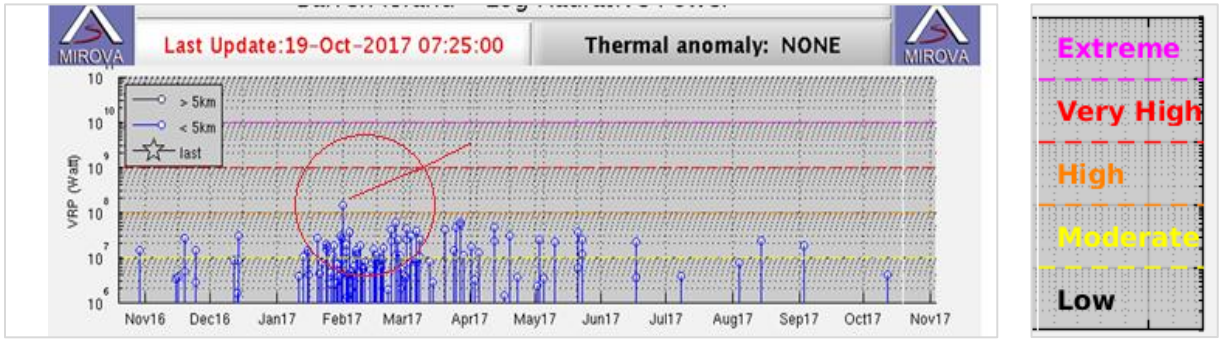

(a) (b)

Figure 5 (a) Log plot of VRP recorded by the MIROVA system for the volcano BIV from November 2016 to November 2017 (Courtesy of MIROVA)

Next second phase of the volcanic unrest period September 2018 to January 2019 considered for monitoring BIV volcano based on thermal anomalies. The LST maps created for the study area BIV during the volcanic disturbance period of September 2018 to January 2019 are shown in *Figures 6(a)* and *(b)*. *Figure 7* depicts the log plot of the VRP obtained from the MIROVA system for the volcano BIV between September 2018 and April 2019 (Courtesy of MIROVA). *Figures 6(a)* and *(b)* show that the highest temperature recorded in 2018 was 28.20°C on October 23 and 40.05°C on November 24. It can be observed from *Figure 7* that, the VRP value was moderate on October 23, 2018 and moderate on November 24, 2018. The estimated LST values for the day 23 October 2018 were not mapping with the VRP values provided by the MIROVA system. According to volcano thermal phenomena volcanic activity can be broadly classified into 3 types, (i) low temperature fumaroles, (ii) high temperature fumaroles, and (iii) lava related effects. On 23rd October 2018 volcanic thermal activity due to low temperature fumaroles based on observations, so it will be typically exhalations of moist steam and sulphureous gases from small vents and fissure in the summit regions of volcanoes [16]. So this can be validated by using false colour composite (FCC) image generated by using short wave infrared-2 (SWIR-2 i.e. band 7), SWIR-1 (band 6), and near infrared (NIR i.e. band 5). *Figure 8* shows the FCC image generated using 7, 6, 5 band dataset of Landsat 8 for the study area BIV volcano on the day 23-10-2019. The presence of thermal anomaly can be observed in the FCC image which was indicated using a green line refer the *Figure 8*.

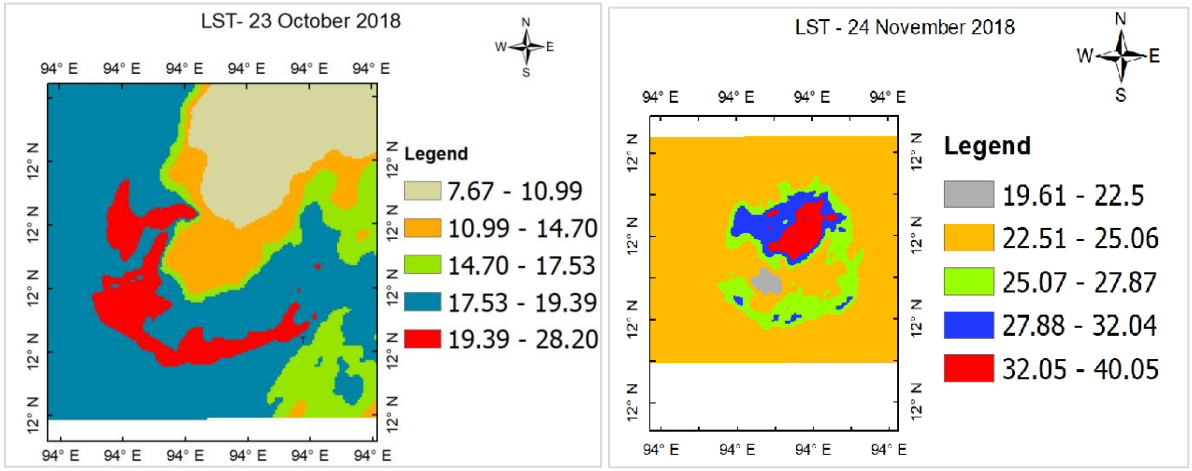

(a) (b)

Figure 6 (a) and (b) LST maps generated for the study area BIV for the volcanic unrest period September 2018 to January, 2019 by taking satellite images of Landsat 8 datasets from USGS earth explorer

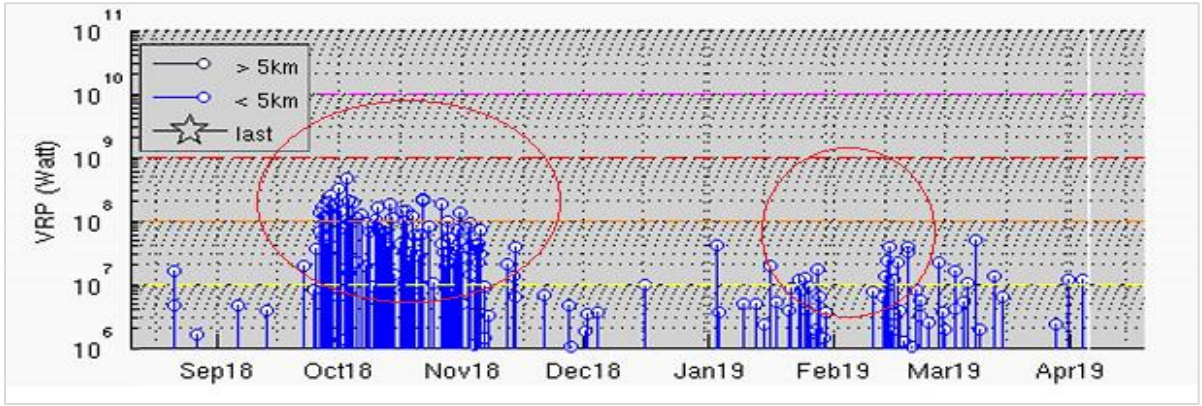

Figure 7 Log plot of VRP recorded by the MIROVA system for the volcano BIV from September 2018 to April 2019 (Courtesy of MIROVA)

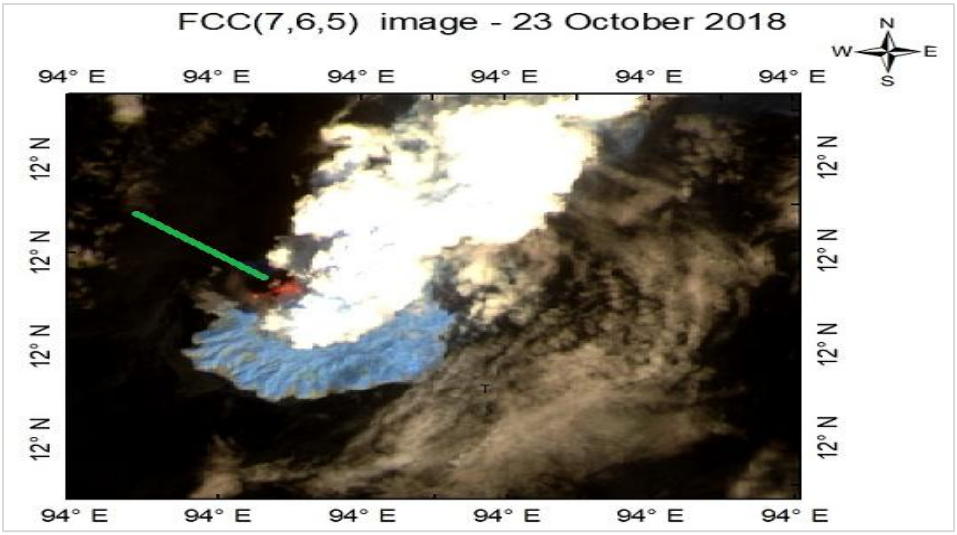

Figure 8 FCC image generated using 7,6,5 band dataset of Landsat 8 for the study area BIV volcano on 23-10-2018

4.2FIRMS (Fire information for resource management system)

In addition to the VRP validation process, other satellite observations from NASA's / NOAA-20 mission having VIIRS sensor data were considered to compare estimated LST numerical. FIRMS is part of NASA's Land, Atmosphere NRT capability for EOS (LANCE). This data based on calibration of active fire products estimated from VIIRS sensor datasets with the resolution of 375m each pixel. The resource to acquire the data is https://firms.modaps.eosdis.nasa.gov/. Temperature values obtained from FIRMS system were used by this research work to validate estimated LST values from Landsat 8 images during unrest periods of the study area BIV volcano. *Table 2* presents the comparison of Landsat 8 based estimated LST values with VIIRS sensor based temperature values at the study area BIV.

Table 2 Comparison of Landsat8 based estimated LST with FIRMS temperatures

Date	Landsat 8	VIIRS
06-02-2017	65.5º C	352K / 79º C
22-02-2017	47.88º C	318 K / 45º C
23-10-2018	28.28º C	300 K / 27º C

The temperatures acquired by both satellite sensors differ by ±10℃ the same can be observed from the *Table 2*. The deviations in the both the measured values may be due variations in acquisition resolutions of the sensors. Each pixel of Landsat 8 has a resolution of 100 metres, while each pixel of VIIRS sensor has a resolution of 375 metres.

4.3 Sentinel-2 datasets

Composite band / FCC images of Sentinel-2 data, such as RGB, SWIR1-NIR-Green, SWIR2-NIR-Green, and SWIR2-SWIR1-NIR band combinations can be used to visually perceive volcanic eruptions at the study area BIV volcano. ArcGIS 10.3 software was used to generate composite band images of the study area using Sentinel-2A &B satellite datasets. When the eruption state is active, the SWIR1 band has high values, and when the eruption state is fading, it has low values. The direction of the lava flow can be identified using FCC images of Sentinel-2 datasets. BIV consists of a north-northeast active polygenetic cone and a west ruptured caldera. A volcanic eruption is described as a shift in a volcano's usual state. Volcanic unrest can manifest itself in a variety of ways, including surface deformation, heat or gas releases, and seismic activity.

This research work considered <10% cloud coverage images of Sentinel-2 datasets. Sentinel-2A & B images can be downloaded from https://earthexplorer.usgs.gov/. Current work considered data for the period of September 2018 to March 2021. Sentinel-2 false color composite images of the study area at various active eruption states at various time periods were shown in *Figure 9*. All Sentinel-2 images of BIV screening, thermal abnormalities, except for the image on date 30-January-2021, which was obscured by smoke and clouds and hence did not show the thermal anomaly. On September 28, 2020, ash has been emitted in the direction of the south-east, north-west on October 3, 2020, and south-west on October 18, 2020. The ash was released nearly to the west of the top crater on

November 11, 2020. Thermal anomalies have not apparent on January 30, 2021, and the direction of lava flow cannot be determined since the flank vent was obscured by clouds and smoke. On February 4, 2021, it was pointing east, while on February 9, 2021, it was pointing towards the south. Ash emissions drifted to the east on February 24, 2021, then to the southwest on March 1, 2021. Therefore, Sentinel-2 datasets are globally used by the volcanic observing systems. MIROVA system also presents the report on the volcanic lava flow direction using Sentinel-2 datasets.

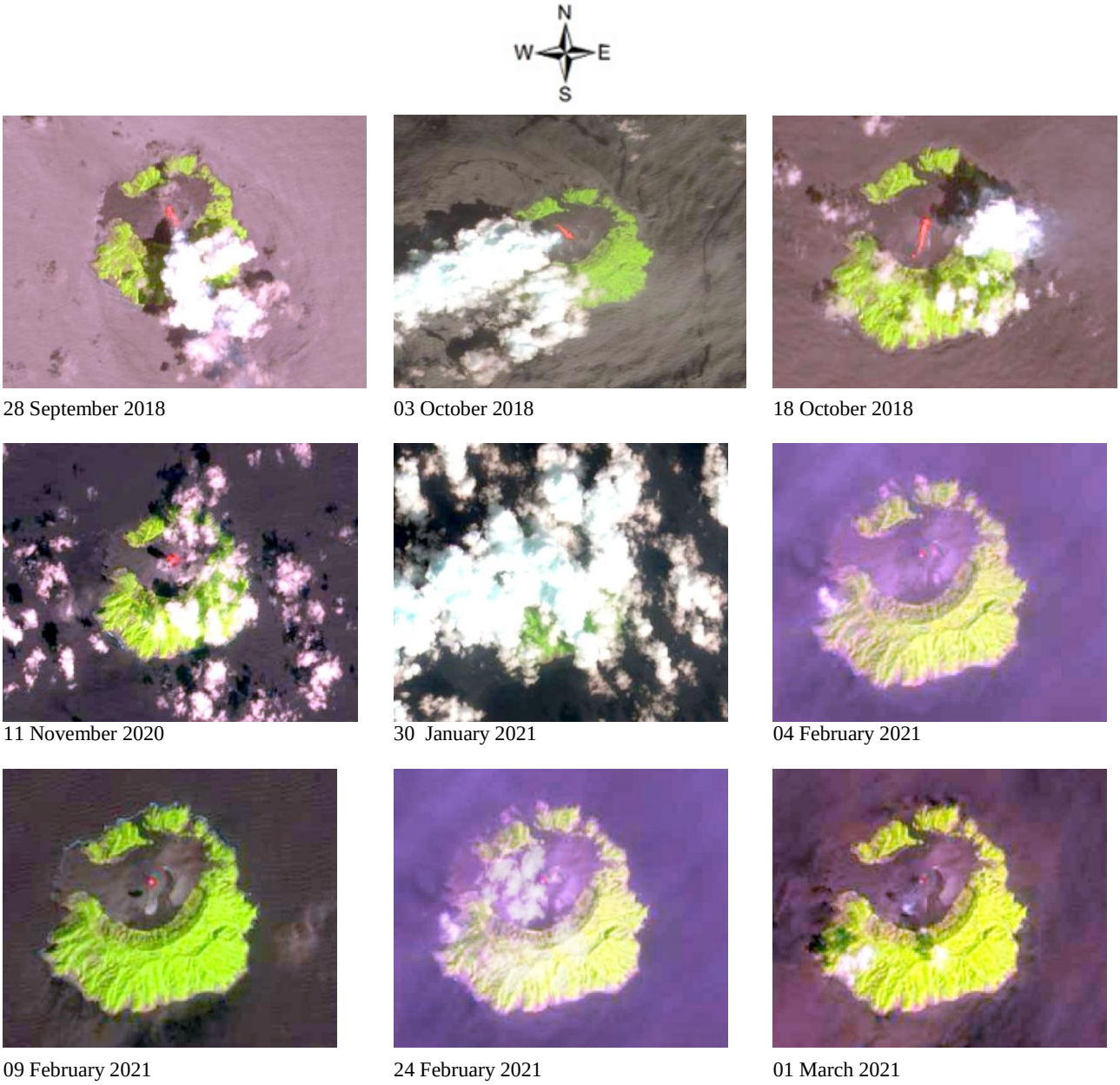

Figure 9 Sentinel-2 FCC images of the study area BIV from September-November, 2018 and November, 2020 to March, 2021 (Source: Sentinel-2 data provided by web resource https://scihub.copernicus.eu/)

4.4Limitation

The goal of the current research is to use thermal remote sensing to track active volcanoes' periods of unrest. It is necessary to receive constant updates on the status of volcanoes at least once a day during critical periods of volcanic eruption. Landsat 8 is unable to consistently deliver data for these applications. Due to the low temporal resolution revisit time 16-day once. This is the primary drawback of Landsat 8 data. Critical times necessitate daily surveillance, which Landsat 8 data cannot provide. The image quality of Landsat8 is also compromised by the cloud of smoke coverage.

A complete list of abbreviations is shown in *Appendix I.*

5.Conclusion and future scope

BIV located in the Andaman Sea, which is India's youngest and most active stratovolcano, with strombolian activity. The current research work focuses on analysing thermal activity using LST parameter. The datasets from Landsat 8 provide changes happening at BIV for the two active phases during January-March, 2017 and September, 2018 to January, 2019. The proposed methodology is to analyse changes occurring at BIV during active phases by utilizing various datasets from multiple sensors and satellites, viz. OLI/TIR – Landsat 8, MSI-Sentinel-2, MODIS-Terra/Aqua, and VIIRS - Suomi NPP / NOAA mission. As volcanic thermal phenomena classified into 3 types (i) low temperature fumaroles, (ii) high temperature fumaroles, and (iii) lava related effects. Based on this phenomenon, from the results interpretation at BIV using LST values both the cases of low temperature and high temperature fumaroles were observed. Multi-sensor and multi-temporal datasets from Landsat 8 (once every 16 days), Sentinel-2 (once every 5 days), and MODIS (4 times a day) considered for monitoring thermal anomalies of volcanoes. Less cloud cover (≤10%) datasets from Landsat 8 and Sentinel-2 were processed. The results interpretation, analysis and validation of obtained LST values were done based on standard resources like MIROVA system, NASA system database.

The results showed a high temperature funeral over the first phase of the unrest period of BIV. While in the second stage of the BIV's disturbance period, fumaroles at both low and high temperatures were seen. So for validation FCC image generated using mid-infrared band data (SWIR-2 & SWIR-1) and near infrared (NIR) band data were considered. It clearly shows the active glowing lava on the vent at the BIV. Finally, both the phase results can be comparable with the log VRP plots provided in the MIROVA system. Further, the FIRMS system based temperature values were compared with the estimated LST values using Landsat 8 datasets. It was observed that there was ±10℃ deviation. The deviation may be due to the two sources having different resolutions of observing the BIV. The unrest periods of active volcanoes can be observed using Sentinel-2 datasets too. This research work also considered the Sentinel-2 data for identification of thermal activity as well as the lava flow direction. Sentinel-2 datasets used to generate FCC images using mid-infrared and near infrared band data having 20m resolution. The resultant FCC images were showing the status of volcano BIV. Validated the results using MIROVA system-based log plots of VRP generated using MODIS datasets. From the results it can be concluded that, estimated LST values and Sentinel-2 based FCC images can have the ability to predict the thermal changes occurring at active volcanoes. The future scope of this work will be extended by evaluating LST values using ASTER data as input and comparing the results to Landsat 8 LST and VIIRS temperature readings.

Acknowledgment

The authors would like to thank USGS Earth Explorer web resource providers for giving access to Landsat 8 images to carry out the present research work. Thanks to the web resource https://scihub.copernicus.eu/ for the Sentinel-2 data. In addition, we want to thank the reviewers and the editors for their comments and suggestions to fine tune the manuscript.

Conflicts of interest

The authors have no conflicts of interest to declare.

Author's contribution statement

A. Rajani: Literature review, data collection, conceptualization, investigation, analysis and interpretation of the results, finally writing manuscript and editing. **S. Varadarajan:** Conceptualization, supervision, manuscript review and editing.

References

[1] Oppenheimer C. Climatic, environmental and human consequences of the largest known historic eruption: Tambora volcano (Indonesia) 1815. Progress in Physical Geography. 2003; 27(2):230-59.

[2] Wright R, Flynn L, Garbeil H, Harris A, Pilger E. Automated volcanic eruption detection using MODIS. Remote Sensing of Environment. 2002; 82(1):135-55.

[3] Wright R, Harris AJ, Torres R, Flynn LP. The effects of volcanic eruptions observed in satellite images: examples from outside the north pacific region. In monitoring volcanoes in the north pacific 2015 (pp. 323-54). Springer, Berlin, Heidelberg.
[4] Dehn J, Dean K, Engle K. Thermal monitoring of North Pacific volcanoes from space. Geology. 2000; 28(8):755-8.
[5] Barsi JA, Schott JR, Hook SJ, Raqueno NG, Markham BL, Radocinski RG. Landsat-8 thermal infrared sensor (TIRS) vicarious radiometric calibration. Remote Sensing. 2014; 6(11):11607-26.
[6] Lowenstern JB, Wallace K, Barsotti S, Sandri L, Stovall W, Bernard B, et al. Guidelines for volcano-observatory operations during crises: recommendations from the 2019 volcano observatory best practices meeting. Journal of Applied Volcanology. 2022; 11(1):1-24.
[7] Mia MB, Fujimitsu Y, Nishijima J. Thermal activity monitoring of an active volcano using Landsat 8/OLI-TIRS sensor images: a case study at the Aso volcanic area in southwest Japan. Geosciences. 2017; 7(4):1-15.
[8] Thompson G, Beer M, Kougioumtzoglou IA, Patelli E, Au SK. Seismic monitoring of volcanoes. Encyclopedia of Earthquake Engineering. 2015; 10:1-25.
[9] Bluth GJ, Rose WI, Sprod IE, Krueger AJ. Stratospheric loading of sulfur from explosive volcanic eruptions. The Journal of Geology. 1997; 105(6):671-84.
[10] Zuo M, Zhou T, Man W, Chen X, Liu J, Liu F, et al. Volcanoes and climate: sizing up the impact of the recent Hunga Tonga-Hunga Ha'apai volcanic eruption from a historical perspective. Advances in Atmospheric Sciences. 2022.
[11] Gupta RK, Badarinath KV. Volcano monitoring using remote sensing data. International Journal of Remote Sensing. 1993; 14(16):2907-18.
[12] Gunda GK, Champatiray PK, Chauhan M, Chauhan P, Ansary M, Singh A, et al. Modelling of volcanic ash with HYSPLIT and satellite observations: a case study of the Barren Island volcano eruption event, Andaman Territory, India. Current Science. 2021; 121(4):529-38.
[13] Jousset P, Pallister J, Boichu M, Buongiorno MF, Budisantoso A, Costa F, et al. The 2010 explosive eruption of Java's Merapi volcano—a '100-year'event. Journal of Volcanology and Geothermal Research. 2012; 241:121-35.
[14] Cigna F, Tapete D, Lu Z. Remote sensing of volcanic processes and risk. Remote Sensing. 2020; 12(16):1-17.
[15] Harris A. Thermal remote sensing of active volcanoes: a user's manual. Cambridge University Press; 2013.
[16] Bhattacharya A, Reddy CS, Srivastav SK. Remote sensing for active volcano monitoring in Barren Island, India. Photogrammetric Engineering and Remote Sensing (United States). 1993; 59(8).
[17] Warwick R, Williams-jones G, Kelman M, Witter J. A scenario-based volcanic hazard assessment for the mount meager volcanic complex, British Columbia. Journal of Applied Volcanology. 2022; 11(1):1-22.
[18] Richter N, Favalli M, De ZDE, Fornaciai A, Da SFRM, Pérez NM, et al. Lava flow hazard at Fogo Volcano, Cabo Verde, before and after the 2014–2015 eruption. Natural Hazards and Earth System Sciences. 2016; 16(8):1925-51.
[19] Martha TR, Roy P, Vinod KK. Lava flows and cinder cones at Barren Island volcano, India (2005–2017): a spatio-temporal analysis using satellite images. Bulletin of Volcanology. 2018; 80(2):1-8.
[20] Coppola D, Laiolo M, Cigolini C, Delle DD, Ripepe M. Enhanced volcanic hot-spot detection using MODIS IR data: results from the MIROVA system. Geological Society, London, Special Publications. 2016; 426(1):181-205.
[21] Prakash S, Norouzi H. Land surface temperature variability across India: a remote sensing satellite perspective. Theoretical and Applied Climatology. 2020; 139(1):773-84.
[22] Patrick M, Dean K, Dehn J. Active mud volcanism observed with Landsat 7 ETM+. Journal of Volcanology and Geothermal Research. 2004; 131(3-4):307-20.
[23] Zaini N, Yanis M, Isa M, Van DMF. Assessing of land surface temperature at the Seulawah Agam volcano area using the Landsat series imagery. In journal of physics: conference series 2021 (pp. 1-7). IOP Publishing.
[24] Pritchard ME, Simons M. An in SAR-based survey of volcanic deformation in the central Andes. Geochemistry, Geophysics, Geosystems. 2004; 5(2).
[25] Vieira D, Teodoro A, Gomes A. Analyzing land surface temperature variations during Fogo Island (Cape Verde) 2014-2015 eruption with Landsat 8 images. In earth resources and environmental remote sensing/GIS applications VII 2016 (pp. 32-45). SPIE.
[26] Campus A, Laiolo M, Massimetti F, Coppola D. The transition from MODIS to VIIRS for global volcano thermal monitoring. Sensors. 2022; 22(5):1-24.
[27] Newhall CG, Costa F, Ratdomopurbo A, Venezky DY, Widiwijayanti C, Win NT, et al. WOVOdat–an online, growing library of worldwide volcanic unrest. Journal of Volcanology and Geothermal Research. 2017; 345:184-99.
[28] Yang M, Zhao W, Zhan Q, Xiong D. Spatiotemporal patterns of land surface temperature change in the tibetan plateau based on MODIS/Terra daily product from 2000 to 2018. IEEE Journal of Selected Topics in Applied Earth Observations and Remote Sensing. 2021; 14:6501-14.
[29] Voogt JA, Oke TR. Thermal remote sensing of urban climates. Remote Sensing of Environment. 2003; 86(3):370-84.
[30] Li ZL, Tang BH, Wu H, Ren H, Yan G, Wan Z, et al. Satellite-derived land surface temperature:

current status and perspectives. Remote Sensing of Environment. 2013; 131:14-37.
[31] Li W, Cao Q, Lang K, Wu J. Linking potential heat source and sink to urban heat island: heterogeneous effects of landscape pattern on land surface temperature. Science of the Total Environment. 2017; 586:457-65.
[32] Arnfield AJ. Two decades of urban climate research: a review of turbulence, exchanges of energy and water, and the urban heat island. International Journal of Climatology: A Journal of the Royal Meteorological Society. 2003; 23(1):1-26.
[33] Guha S, Govil H, Diwan P. Monitoring LST-NDVI relationship using Premonsoon Landsat datasets. Advances in Meteorology. 2020.
[34] Yuan X, Wang W, Cui J, Meng F, Kurban A, De MP. Vegetation changes and land surface feedbacks drive shifts in local temperatures over Central Asia. Scientific Reports. 2017; 7(1):1-8.
[35] Dash P, Göttsche FM, Olesen FS, Fischer H. Land surface temperature and emissivity estimation from passive sensor data: theory and practice-current trends. International Journal of Remote Sensing. 2002; 23(13):2563-94.
[36] Rajani A, Varadarajan S. Estimation and validation of land surface temperature by using remote sensing & GIS for chittoor district, Andhra Pradesh. Turkish Journal of Computer and Mathematics Education. 2021; 12(5):607-17.
[37] Luintel N, Ma W, Ma Y, Wang B, Subba S. Spatial and temporal variation of daytime and nighttime MODIS land surface temperature across Nepal. Atmospheric and Oceanic Science Letters. 2019; 12(5):305-12.
[38] Gunda GK, Ray PK, Chauhan M, Chauhan P, Balaji S. Barren Island volcanism and seismicity: an intriguing finding. Journal of Earth System Science. 2021; 130(3):1-19.
[39] Coppola D, Laiolo M, Cigolini C, Massimetti F, Delle DD, Ripepe M, et al. Thermal remote sensing for global volcano monitoring: experiences from the MIROVA system. Frontiers in Earth Science. 2020; 7:1-21.
[40] Blackett M. Early analysis of Landsat-8 thermal infrared sensor imagery of volcanic activity. Remote Sensing. 2014; 6(3):2282-95.
[41] Flynn LP, Harris AJ, Wright R. Improved identification of volcanic features using Landsat 7 ETM+. Remote Sensing of Environment. 2001; 78(1-2):180-93.
[42] Ramsey MS, Harris AJ. Volcanology 2020: how will thermal remote sensing of volcanic surface activity evolve over the next decade? Journal of Volcanology and Geothermal Research. 2013; 249:217-33.
[43] Ramsey MS, Flynn IT. The spatial and spectral resolution of ASTER infrared image data: a paradigm shift in volcanological remote sensing. Remote Sensing. 2020; 12(4):1-40.
[44] Silvestri M, Rabuffi F, Pisciotta A, Musacchio M, Diliberto IS, Spinetti C, et al. Analysis of thermal anomalies in volcanic areas using multiscale and multitemporal monitoring: vulcano island test case. Remote Sensing. 2019; 11(2):1-32.
[45] Marchese F, Genzano N, Neri M, Falconieri A, Mazzeo G, Pergola N. A multi-channel algorithm for mapping volcanic thermal anomalies by means of Sentinel-2 MSI and Landsat-8 OLI data. Remote Sensing. 2019; 11(23):1-25.
[46] Layana S, Aguilera F, Rojo G, Vergara Á, Salazar P, Quispe J, et al. Volcanic Anomalies monitoring System (VOLCANOMS), a low-cost volcanic monitoring system based on Landsat images. Remote Sensing. 2020; 12(10):1-32.
[47] Xiang J, Guo S, Shi X, Yu D, Wei G, Wen N, et al. Revealing the morphological evolution of krakatau volcano by integrating SAR and optical remote sensing images. Remote Sensing. 2022; 14(6):1-11.
[48] Cho D, Bae D, Yoo C, Im J, Lee Y, Lee S. All-Sky 1 km MODIS land surface temperature reconstruction considering cloud effects based on machine learning. Remote Sensing. 2022; 14(8):1-20.
[49] Biggs J, Dogru F, Dagliyar A, Albino F, Yip S, Brown S, et al. Baseline monitoring of volcanic regions with little recent activity: application of Sentinel-1 In SAR to Turkish volcanoes. Journal of Applied Volcanology. 2021; 10(1):1-4.
[50] Gunda GK, Champatiray PK, Chauhan M, Chauhan P. Monitoring of volcanic eruption (Barren Island) using EO satellites. Current Science. 2020; 118(12):1874-6.
[51] Poland MP, Lopez T, Wright R, Pavolonis MJ. Forecasting, detecting, and tracking volcanic eruptions from space. Remote Sensing in Earth Systems Sciences. 2020; 3(1):55-94.
[52] Hooper A, Prata F, Sigmundsson F. Remote sensing of volcanic hazards and their precursors. Proceedings of the IEEE. 2012; 100(10):2908-30.
[53] Mal S, Rani S, Maharana P. Estimation of spatio-temporal variability in land surface temperature over the Ganga River Basin using MODIS data. Geocarto International. 2020; 37(13):3817-39.
[54] Sattari F, Hashim M. A brief review of land surface temperature retrieval methods from thermal satellite sensors. Middle-East Journal of Scientific Research. 2014; 22(5):757-68.

A. Rajani, is a Research Scholar (part-time) in the Department of Electronics and Communication Engineering at Sri Venkateswara University College of Engineering, Tirupati, India. She has obtained her B.E (ECE) from Osmania University, Hyderabad in 2001 and M.Tech in Electronic Instrumentation and Communication Systems from Sri Venkateswara University, Tirupati in 2010. She has 12 years of teaching experience. Her research areas of interest include Image

Processing, Signal Processing and Embedded Systems and Microcontrollers. She has published more than 16 papers in national and international journals. She is a member of the Institute of Engineers (India). Currently working as an Assistant Professor at Annamacharya Institute of Technology and Sciences, Tirupati, Andhra Pradesh, India.
Email: rajanisvu2015@gmail.com

Dr. S. Varadarajan is working as a Professor in the department of Electronics and Communication Engineering at Sri Venkateswara University college of Engineering, Tirupati, Andhra Pradesh, India. He has 25 years of teaching experience. He received his Ph.D. from Sri Venkateswara University, Tirupati, AP, India. His areas of interest are Digital Communication, Image and Signal Processing. He has published more than 100 papers in national and international conferences and national and international journals. He is a Fellow of the Andhra Pradesh Academy of Sciences (FAPAS), Fellow of IETE and IE. He chaired and served as reviewer for several international conferences and is a member of the editorial board of several international conferences and is a member of the editorial board of several international journals. He visited the USA and UK. He worked as a secretary, Andhra Pradesh State Council of Higher Education from January 2016 to August 2019.
Email: svaradarajan@svuniversity.edu.in

Appendix I

S. No.	Abbreviation	Description
1	ALI	Advanced Land Imager
2	ALOS-2	Advanced Land Observation Satellite-2
3	ArcGIS	Aeronautical Reconnaissance Coverage Geographic Information System
4	ASTER	Advanced Spaceborne Thermal Emission and Reflection Radiometer
5	BIV	Barren Island Volcano
6	CVGHM	Center for Volcanology and Geologic Hazard Mitigation
7	DN	Digital Number
8	DNB	Day/Night Band
9	EO-1	Earth Observing one
10	EOS	Earth Observing System
11	ESA	European Space Agency
12	ETM+	Enhanced Thematic Mapper Plus
13	FCC	False Color Composite
14	FIRMS	Fire Information for Resource Management System
15	GPS	Global Positioning System
16	GVP	Global Volcanism Programme
17	InSAR	Interferometric Synthetic Aperture Radar
18	ISRO	Indian Space Research Organization
19	LANCE	Land Atmosphere Near real-time capability for EOS
20	LDAPS	Local Data Assimilation and Prediction System
21	LightGBM	Light Gradient Boosting Machine
22	LSE	Land Surface Emissivity
23	LST	Land Surface Temperature
24	MIROVA	Middle InfraRed Observation of Volcanic Activity
25	MODIS	Moderate Resolution Imaging Spectroradiometer
26	MSI	Multi-Spectral Imager
27	MSL	Mean Sea Level
28	NASA	National Aeronautics and Space Administration
29	NDVI	Normalized Difference Vegetation Index
30	NHI	Normalized Hotspot Index
31	NIO	National Institute of Oceanography
32	NIR	Near InfraRed
33	NOAA	National Oceanic and Atmospheric Administration
34	NPP	National Polar-orbiting Partnership
35	NRT	Near Real Time
36	OLI	Operational Land Imager
37	RHF	Radiative Heat Flux
38	ROI	Region of Interest
39	RSO	Remote Sensing Observations
40	SAR	Synthetic Aperture Radar
41	SD	Standard Deviation
42	SDWI	Sentinel-1 Dual-Polarized Water Index
43	SWIR	Short Wave InfraRed
44	TIRS	Thermal InfraRed Sensor
45	TM	Thematic Mapper
46	TOA	Top of Atmosphere
47	TROPOMI	TROPOspheric Monitoring Instrument
48	TVG	Tatun Volcanic Group
49	USGS	United States Geological Survey
50	VAAC	Volcanic Ash Advisory Center
51	VDAP	Volcano Disaster Assistance Program
52	VIIRS	Visible Infrared Imaging Radiometer Suite
53	VIPS	Volcanic Image Processing Software
54	VOLCANOMS	Volcanic Anomalies Monitoring System
55	VRP	Volcanic Radiative Power
56	WOVO	World Organization of Volcano Observatories
57	WRS-2	Worldwide Reference System-2